

**RIGA TECHNICAL UNIVERSITY**

**Katrina BOLOCHKO**

**THREE-DIMENSIONAL MEDICAL IMAGE CONSTRUCTION  
AND PROCESSING**

**Summary of doctoral thesis**

**Riga 2011**

**RIGA TECHNICAL UNIVERSITY**  
Faculty of Computer Science and Information Technology  
Institute of Computer Control, Automation and Computer  
Engineering

**Katrina BOLOCHKO**

Automation and Computer Engineering Doctoral Programm Doctoral Student

**THREE-DIMENSIONAL MEDICAL IMAGE CONSTRUCTION  
AND PROCESSING**

**Summary of doctoral thesis**

Supervisor  
Dr. habil. sc. ing., professor  
**A.GLAZS**

**Riga 2011**

UDK 004.932+616-073.7](043.2)  
Bo 364 t

Bolochko K.  
THREE-DIMENSIONAL MEDICAL IMAGE  
CONSTRUCTION AND PROCESSING. -  
R.:RTU, 2011.-33 pp.

Issued in compliance with ICCACE decision of  
March 4, 2011, Protocol Nr.98

This work has been supported by the European  
Social Fund within the National Programme  
"Support for the carrying out doctoral study  
programm and post-doctoral researches" project  
"Support for the development of doctoral  
studies at Riga Technical University".

**ISBN 978-9934-10-198-4**

**DOCTORAL THESIS  
PROPOSED TO OBTAIN THE DEGREE OF DOCTOR  
FROM RIGA TECHNICAL UNIVERSITY**

Doctoral thesis in engineering sciences is proposed to obtain the degree of Doctor from Riga Technical University and in accordance with the decision of the Doctorate Board, the public defence shall be held on October 3, 2011, 14.00 at the Faculty of Computer Science and Information Technology, Meza Str. 1/3, room 202.

**OFFICIAL OPPONENTS**

Professor, Dr.habil.sc.ing. Janis Grundspenkis  
Riga Technical University

Professor, Dr.habil.sc.ing, Peteris Rivza  
Latvia University of Agriculture

Professor, Dr.habil.sc.ing, Arunas Lukosevicius  
Kaunas University of Technology, Lithuania

**ORIGINALITY STATEMENT**

I hereby declare that the work presented in this thesis is my own and has been proposed to obtain the degree of Doctor in engineering sciences at Riga Technical University. This thesis contains no material, which has been accepted for the award of any other degree or diploma at RTU or any other educational institution.

Katrina Bolochko .....(Signature)

Date: .....

The Doctoral thesis written in Latvian, consists of introduction, 4 chapters, conclusion, list of literature, 1 appendix, 98 drawings and illustrations, total number of pages is 144. The list of literature contains 96 headlines.

## CONTENTS

1.	GENERAL CHARACTERIZATION OF THE DOCTORAL THESIS .....	5
1.1.	Topic actuality .....	5
1.2.	The aim and tasks of the doctoral thesis .....	6
1.3.	The field and object of research .....	7
1.4.	Scientific novelty of the doctoral thesis .....	7
1.5.	Practical significance of the doctoral thesis .....	7
1.6.	The structure of the doctoral thesis.....	10
2.	CONTENTS OF THE DOCTORAL THESIS .....	11
2.1.	2D medical images and their processing .....	11
2.2.	3D medical image modeling.....	12
2.3.	Medical image processing and visualization methods .....	13
2.4.	Medical image processing methods approbation.....	22
3.	RESULTS AND CONCLUSIONS .....	30
	REFERENCES .....	32

# 1. GENERAL CHARACTERIZATION OF THE DOCTORAL THESIS

## 1.1. Topic actuality

Image processing (quality enhancement, region of interest selection, etc.) and three-dimensional (3D) image modeling and visualization is an actual theme in various fields. For example, in medicine, criminalistics, geology it is very important to extract informative regions from the image, because they help make decisions on image classification. For instance, when analyzing medical images that are acquired using Computer Tomography (CT) or Magnetic Resonance Imaging (MRI), only partial information is required from the image (pathology zone). In criminalistics, in order to identify a person, only a fragment of the whole image is necessary (person's face). Therefore, it is important to extract from the images such regions of interest that would provide most information for classification tasks.

On the other hand, sometimes two-dimensional (2D) representation of the images or regions is not enough for image analysis and classification. Three-dimensional (3D) image visualization provides greater resources for image or region analysis.

In this work, image processing and 3D visualization tasks are solved using the medical images of a brain as input data, although the proposed methods can be adapted for other images as well. Medical images that are acquired with help of computer tomography or magnetic resonance imaging are widely used in diagnostics. Processing and analysis of such images is an actual task in both scientific field, as it allows the research of medical image structures, and clinical field, as it can help physicians diagnose the patient.

Image processing is a complicated problem in biomedical engineering, because the majority of medical images have low contrast, low quality and high complexity in image structures. To ease the medical image analysis for the physicians, it is necessary to solve such medical image processing tasks as image segmentation, region of interest (pathology zone) extraction, 3D visualization, region of interest (pathology zone) volume estimation, etc.

One of the first steps in medical image processing is image segmentation. There are many existing manual, semi-automatic and automatic segmentation algorithms, but most of them are not specifically designed for medical image segmentation. In order to process medical images correctly, the algorithms must work with substance's density, not pixel intensities, that is why specialized medical image algorithms are being developed. Some of the specialized segmentation algorithms are described in different scientific publications [2, 8, 11, 12, 16], but these algorithms have several disadvantages. They are complex in use, or do not provide any additional data about substances in medical images. Several algorithms have too many parameters that need to be adjusted for each specific image. For example, algorithm described in [17] requires the user to input the resulting segment count. But for every medical image this number can be different. Therefore, the physician must experimentally decide what segment count number would be best for each specific image. This, in turn, can complex the task of diagnostics for the physician. Also, manual segmentation methods require more time from the user, on the other hand, automatic algorithms cannot be used without the supervision of the physician, because only physicians should make the final decision about the pathologies in medical images. Therefore, it is necessary to create a semi-automatic segmentation algorithm that would work quickly and provide the physician with information about each segment and its substances. The segmentation algorithm should also be easy to use.

The second image processing step after image segmentation, is region of interest (for example, pathology zone) extraction and analysis. In medical imaging, this means finding the

region's length, width, volume, type of substance, etc. One of the most important tasks is the measuring of the pathology zone's volume. Although there are several algorithms that allow measurement of the pathology zone [3, 4, 9, 15], they work with 2D data – medical image slices and do not take into account the object's 3D structure. This can lead to imprecision in volume measurements. Therefore, it is necessary to assess the precision of the 2D volume estimation methods, as well as test the algorithm that would use 3D data for volume estimation.

The process of creating a 3D object from 2D medical image data set is another important task of medical diagnostics. 3D visualization of medical images can help physicians see the pathology zone's exact position and plan necessary medical operations. Because the 3D object is created from 2D data set, the visualization consists of two tasks. Firstly, in order to obtain the 3D representation of the region of interest, it is necessary to find control points on the region of interest on each medical image slice. Secondly, from the obtained control points it is necessary to form a 3D surface that can then be visualized. The existing control point finding algorithms have several disadvantages such as low precision or a great number of control points that can result in slow data visualization. This leads to the task of finding the minimal number of control points that would allow precise interpolation of the region of interest's contour. Visualization methods in medicine are using raster methods for 3D object creation – each pixel (point) of the image is displayed in 3D as a voxel (pixel's representation in 3D). But the quality of the created 3D object is very low. Vector methods, on the other hand, use surfaces or polygons to describe the 3D object. Existing vector methods have some disadvantages, like an aliasing effect or heterogeneity of the resulting surface. Therefore, it is necessary to develop a visualization algorithm that would be able to provide a better quality of the 3D model.

All abovementioned methods usually are combined into one medical image processing system. There are different systems that have necessary processing and analysis tools in modern tomography, but such systems can be only installed on computers that are linked to the tomography. It is not always possible to conduct medical image analysis on this computer, since it mostly used for scanning patients. On the other hand, independent medical image processing systems [1] are not able to provide all the necessary tools for medical image processing and analysis tasks. Such disadvantages of specialized and independent medical image processing systems lead to the necessity of developing a new medical image processing system that would be both independent from the tomography and could provide necessary tool for medical image analysis.

## **1.2. The aim and tasks of the doctoral thesis**

**The aim of the doctoral thesis** is to develop methods for medical image processing (image segmentation, region of interest extraction, medical object 3D visualization, etc) and combine the developed methods into one medical image processing system. In order to achieve this aim it is first necessary to understand what image processing tools are required for medical images. According to the dean of Faculty of Medicine from Riga Stradina University and Gailezers hospital Radiology department director prof., Dr.med. A. Platkajis, the necessary methods that must be implemented in the image processing system can be described as follows:

- ability to extract any region of interest from medical images
- ability to estimate the extracted zone's size (length, width) and volume of the region of interest;
- system must be able to visualize the pathology zone and persons head in 3D, so physicians could see the zone's exact position and plan necessary operations;

- ability to automatically analyze the pathology zone's substance as well as substance around it and provide this information to the physician.

Therefore, according to the abovementioned requirements in order to achieve the aim of this work it is necessary to solve the following **tasks of the doctoral thesis**:

- provide the ability to analyze medical images in standard graphical formats and in DICOM format;
- develop methods for medical image segmentation and region of interest extraction;
- develop methods of medical image 3D visualization;
- develop methods of volume estimation of the extracted region;
- develop methods for medical image pre-processing and substance analysis.

### **1.3. The field and object of research**

The field of research in doctoral thesis are the medical image processing algorithms. The doctoral thesis analyses such image processing methods as image segmentation, region of interest extraction, medical object 3D visualization, and region of interest volume estimation.

The object of research in doctoral thesis is a data set of 2D medical images (slices) that form a 3D structure of the patient's brain. The analysis of this 3D structure is achieved through processing of 2D images. The images were acquired by means of computer tomography and magnetic resonance and were provided by dean of Faculty of Medicine from Riga Stradina University and Gailezers hospital Radiology department director prof., Dr.med. A. Platkajis.

### **1.4. Scientific novelty of the doctoral thesis**

New achievements are:

1. Developed semi-automatic medical image segmentation and region extraction methods that don't have the existing methods disadvantages.
2. Developed control point finding method for further 3D modeling. In contradiction to existing methods, the developed method provides the minimal number of points necessary to interpolate the contour precisely.
3. Developed method of 3D modeling for further visualization. The method takes into account the specifics of medical images and combines the obtained control points into a surface that can be the visualized using standard OpenGL library.
4. Developed method of medical object volume estimation that uses 2D medical images as input data. Experimentally proven that it is more precise than the existing methods. There were also experiments conducted with an existing method of volume estimation that uses 3D object data as input data (Sisojevs, 2009) [13, 14].

### **1.5. Practical significance of the doctoral thesis**

The practical significance of the work is the developed medical image processing system that includes all developed image processing methods and can be used for analysis of medical images obtained with computer tomography. This system can help physicians analyze medical images and provide information necessary for a correct and timely

diagnostics. Such tools as medical image segmentation and volume estimation will allow physicians to measure the volume of pathology zone and analyze its substance.

The results of this work were presented in 14 scientific conferences and published in 15 scientific publications.

### **Publications:**

1. Krechetova K., Glazs A., Lubans A. A Modified Algorithm for Medical Image Segmentation // Biomedical Engineering. Proceedings of International Conference, 9th Annual International Biomedical Engineering Conference, Lietuva, Kaunas, 27.-28. oktobris, 2005, pp. 256-259
2. Krečetova K., Glazs A., Lubāns A. Modificēts algoritms medicīnas attēlu segmentācijai // RTU zinātniskie raksti. 5. sēr., Datorzinātne. - 24. sēj., 2005, pp. 25-30
3. Krechetova K., Glazs A. Development of a New Segmentation Method for Medical Images // Biomedical Engineering. Proceedings of International Conference, 11th Annual International Biomedical Engineering Conference, Lietuva, Kaunas, 25.-26. oktobris, 2007, pp. 133-136
4. Krečetova K., Glazs A. Jaunas medicīnas attēlu segmentācijas metodes izstrādāšana // RTU zinātniskie raksti. 5. sēr., Datorzinātne. - 32. sēj. 2007, pp. 14-21
5. Krechetova K., Glazs A., Platkajis A. 3D Medical Image Visualization and Volume Estimation of Pathology Zones // IFMBE Proceedings. NBC - 14th Nordic-Baltic Conference on Biomedical Engineering and Medical Physics, Latvija, Riga, 16.-20. jūnijs, 2008, pp. 532-535 (*indexed by SpringerLink, Scopus*)
6. Krechetova K., Glazs A. Pathology Zone Volume Estimation in 3D Medical Images of a Brain // Biomedical Engineering. Proceedings of International Conference, 12th Annual International Biomedical Engineering Conference, Lietuva, Kaunas, 23.-24. oktobris, 2008, pp. 225-228
7. Krechetova K., Glazs A. Patoloģijas zonu tilpuma noteikšana 3D medicīnas attēlos // RTU zinātniskie raksti. 5. sēr., Datorzinātne. - 35. sēj. 2008, pp. 18-26 (*indexed by Ebscohost in Computers & Applied Sciences Complete*)
8. Krechetova K., Glazs A. Volume Estimation of Pathology Zones in 3D Medical Images // IFMBE Proceedings. 4th European Conference of the International Federation for Medical and Biological, Beļģija, Antwerp, 23.-27. novembris, 2008, pp. 617-620 (*indexed by SpringerLink, Scopus*)
9. Sisojevs A., Krechetova K., Glazs A. 3D Modeling of Free-Form Object (Interpolation, Visualization and Volume Estimation) // The 17th International Conference on Computer Graphics, Visualization and Computer Vision WSCG'2009 Communication Papers proceedings. – Plzen: University of West Bohemia, 2009, pp. 125-128 (*indexed by Thompson Reuters ISI, available at WSCG Digital Library*)
10. Krechetova K., Glazs A. Contour Extraction and Processing in CT Images // Biomedical Engineering. Proceedings of International Conference, 13th Annual International Biomedical Engineering Conference, Lietuva, Kaunas, 29.-30.oktobrī, 2009 (*available at Kaunas University of Technology Biomedical Engineering Institute website - www.bmii.ktu.lt*)
11. Krečetova K., Glazs A., Slimības diagnostika pēc datortomogrāfijas datiem // RTU zinātniskie raksti. 5. sēr., Datorzinātne. - 39. sēj. 2009, 8.-14. lpp. (*indexed by Ebscohost in Computers & Applied Sciences Complete*)

12. Krechetova K., Sisojevs A., Glazs A., Platkajis A. Medical Image Region Extraction and 3D Modeling Based on Approximating Curves // International journal of Advanced Materials Research (ISSN: 1022-6680) edited by Trans. Tech. Publications Ltd, Switzerland, 2009 (*indexed by EI Compendex, available at Scientific.Net*)
13. Bolochko K., Glazs A. Contour Processing and 3D Visualization in Medical Images // Biomedical Engineering. Proceedings of International Conference, 14th Annual International Biomedical Engineering Conference, Lietuva, Kaunas, 28.-29.oktobrī., 2010, 216.-219. pp. (*available at Kaunas University of Technology Biomedical Engineering Institute website - www.bmii.ktu.lt*)
14. Boločko K., Glazs A. Trīsdimensiju modeļa izveidošana balstoties uz kontūriem medicīnas attēlos // RTU zinātniskie raksti. 5. sēr., Datorzinātne, 2010. (*indexed by Ebscohost in Computers & Applied Sciences Complete*).
15. Bolochko K., Kovalovs M., Glaz A., Medical Image 3D Visualization by Vector Based Methods // IADIS Multi Conference on Computer Science and Information Systems, Computer Graphics, Visualization, Computer Vision and Image Processing, 24-26 July, 2011 (*accepted for publishing*)

#### **Presentations in conferences:**

1. RTU 46. Starptautiskā zinātniskā konference. Rīga, 13.-15. oktobris, 2005.
2. 9th Annual International Biomedical Engineering Conference, Lithuania, Kaunas, 27.-28. October, 2005.
3. RTU 48. Starptautiskā zinātniskā konference. Rīga, 11.-13. oktobris, 2007.
4. 11th Annual International Biomedical Engineering Conference, Lithuania, Kaunas, 25.-26. October, 2007.
5. 2nd International Conference on Actual Problems of Biomedical Engineering, Informatics, Cybernetics and Telemedicine, Ukraine, Kiev, 15.-17. November, 2007.
6. 14th Nordic-Baltic Conference on Biomedical Engineering and Medical Physics, Latvia, Riga, 16.-20. June, 2008.
7. RTU 49. Starptautiskā zinātniskā konference. Rīga, 13.-15. oktobris, 2008.
8. Biomedical Engineering, 12th Annual International Biomedical Engineering Conference, Lithuania, Kaunas, 23.-24. October, 2008.
9. 4th European Conference of the International Federation for Medical and Biological Engineering, Antwerp, Belgium, 23.-28. November, 2008.
10. RTU 50. Starptautiskā zinātniskā konference. Rīga, 12.-16. oktobris, 2009.
11. Biomedical Engineering, 13th Annual International Biomedical Engineering Conference, Lithuania, Kaunas, 29.-30. October, 2009.
12. The 9th International Conference on Global Research and Education Inter-Academia 2010, Riga, Latvia, August 9-12, 2010.
13. RTU 51. Starptautiskā zinātniskā konference. Rīga, 13.-17. oktobris, 2010.
14. Biomedical Engineering, 14th Annual International Biomedical Engineering Conference, Lithuania, Kaunas, 30.-31. October, 2010.

#### **Awards:**

1. Laureate diploma for first place in the 11<sup>th</sup> International conference «Biomedical Engineering» Young Investigators Competition, organised by Kaunas University of Technology for the paper entitled «Development of a New Segmentation Method for Medical Images», 2007.

2. Finalist diploma IFMBE YIC (Young Investigators Competition) in International conference “4th European Conference of the International Federation for Medical and Biological Engineering”, Antwerp, Belgium for the paper entitled “Volume Estimation of Pathology Zones in 3D Medical Images”, 2008.
3. Laureate diploma for first place in the 13<sup>th</sup> International conference «Biomedical Engineering» Young Investigators Competition, organised by Kaunas University of Technology for the paper entitled «Contour Extraction and Processing in CT Images», 2009.

## 1.6. The structure of the doctoral thesis

The doctoral thesis consists of introduction, 4 chapters, conclusions and references. The structure of the doctoral thesis can be described as follows:

**Introduction** – general characterization of the work. Describes the topic actuality, aim and tasks of the doctoral thesis, field of research, scientific novelty and practical significance of the work.

**1st chapter: 2D medical images and their processing** – describes medical image acquisition principles, medical image storing format and its structure. The chapter also includes image processing methods analysis. Different image quality enhancement and segmentation methods are researched in order to evaluate their results and determine their effectiveness for medical image processing system.

**2nd chapter: 3D medical image modeling** – describes the medical image 3D visualization tasks and 3D model types. The advantages and disadvantages of the model types are analyzed in order to determine the best possible model type for medical image 3D visualization.

**3rd chapter: Medical image processing and visualization methods** – describes the developed methods of medical image processing and visualization that allow solving such medical image processing tasks as segmentation, region extraction, region's volume estimation, 3D visualization, etc. The chapter contains detailed description of the methods and some examples of their result.

**4th chapter: Medical image processing methods approbation** – the chapter describes the experiments that were conducted using the developed methods. The results are also compared with existing methods and advantages of the developed methods are described.

**Results and conclusions of the doctoral thesis**

**References**

## 2. CONTENTS OF THE DOCTORAL THESIS

### 2.1. 2D medical images and their processing

In this chapter the 2D medical image acquisition and storage principles are analyzed with the aim to understand the process of medical image acquisition and the structure of storage format for further analysis and processing. Computer tomography (CT) and magnetic resonance imaging (MRI) systems are described, as well as the process of medical image construction from CT and MRI data. The chapter also includes information about the medical image format DICOM and its file structure. In contradiction to the existing image graphic formats, DICOM format contains information about substance density, instead of pixel intensity and also some additional information, like patient's data, time of scan, physician's data, etc. By analyzing different methods of acquiring medical images (CT, MRI) one must come to the conclusion that different methods of acquisition result in different file structure. The information about the substance density is different for CT and MRI scans, although the main advantage of the DICOM structure is the fact that information is stored in substance densities. For example, in CT scans the density is described by Hounsfield units (HU), some of the HU values for different substances are illustrated by table 2.1.

**2.1. table. Different substance densities in Hounsfield units**

Substance	Density, HU	Substance	Density, HU
Bones	+1000	Gray matter	+20 - 40
Blood clot	+55 - 75	Blood	+13 - 18
Spleen	+50 - 70	Cerebrospinal fluid	+15
Liver	+40 - 70	Tumor	+5 - 35
Pancreatic gland	+40 - 60	Cholecyst	+5 - 30
Kidney	+40 - 60	Water	0
Aorta	+35 - 50	Orbits	-25
Muscles	+35 - 50	Fat	-100
White matter	+36 - 46	Lungs	-150 - 400
Cerebellum	+30	Air	-1000

It should be noted, that additional data included in DICOM file contains a priori information about medical image substances. This allows conducting different operations on medical images that are not possible when using simple graphic formats. For example, it is possible to automatically search for a specific substance on the medical image, by using its exact density range. Therefore, it is important for the medical image processing system to be able to work with DICOM format files.

The chapter describes existing 2D medical image quality enhancement methods with the aim to determine their necessity in the medical image processing system. The conclusion is that the main disadvantage of the image quality enhancement procedure is the possibility to erase important information from the medical image. This is especially crucial for the DICOM medical image format. Every detail of the medical image is significant to the physician and it is important to preserve as many details as possible. Therefore, in this work, medical image quality enhancement methods were not used, in order to preserve the important image information.

Different segmentation algorithms are also described and analyzed in this chapter. The aim of this analysis was to determine the effectiveness of the algorithms for use in the medical image processing system. Several different segmentation algorithm groups were

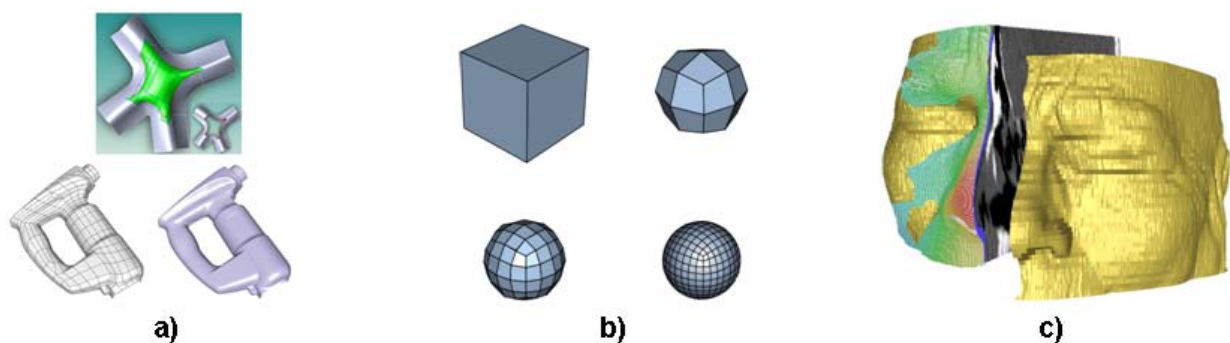
analyzed: edge-based segmentation, region-based segmentation, histogram-thresholding based segmentation and clustering algorithms.

The analysis of the image segmentation algorithm shows that the most efficient segmentation group is the histogram-thresholding segmentation. Edge-based segmentation does not provide any information about regions on the image (for example, pathology zones); it can only be used as an additional tool for visualizing the edges of the selected regions or for edge analysis. Region-based segmentation is oriented toward selecting one specific region and determining the area of the selected region. Clustering methods are rarely used for medical images, they have many additional parameters and results vary under different circumstances. Histogram-thresholding based methods, on the other hand, are fast, efficient and allow quick segmentation of the whole medical image. But existing algorithms have some disadvantages: the initial parameters that need to be set before segmentation begins. The parameters can be sometimes difficult to understand, especially for physicians. For example, an existing method, described in [17] requires the input of the number of resulting segments. Since the physician is not an expert in computer graphics it can be difficult for him to set the correct number of segments in order to, for example, obtain a segment of a pathology zone. And because the pathology zones may vary in density, the optimal number of resulting segments can be different for each medical image. Although it is impossible to avoid such parameters for the medical images in graphic format, the structure of the DICOM file and its additional data allows relieving the physicians from setting the parameters that they don't understand. Therefore, a task emerges, to develop a segmentation method, designed specifically for medical images and would be easy to understand and maintain for physicians.

## 2.2. 3D medical image modeling

First of all, it is important to understand that the data set of 2D medical images forms a 3D structure of the patients scanned organs. The task of 3D modeling, in this case, is to reconstruct this 3D structure from the set of 2D medical images and reproduce this structure in 3D space.

In this chapter the basic 3D model types are analyzed and some of the methods for 3D model visualization quality enhancement (like lighting) are described. In general, there are three types of models in 3D graphics. These are: polygonal models, voxel (raster) models and analytical models (illustrated by figure 2.1).



2.1. fig. a) analytical model, b) polygonal model, c) voxel model.

The analytical model describes the surface of the 3D object with mathematical formulas. The polygonal model consists of such basic elements as vertices, vectors, polylines, polygons and polygon surfaces. Voxel models consist of 3D raster points. Like pixels, that are 2D raster points, forming the 2D image, voxels (volume element) are 3D raster points,

forming the 3D model. It should be noted, that each type of 3D model has its own advantages and disadvantages, which determine their effectiveness in medical image 3D modeling tasks. Polygonal models are defined by good quality, and a small amount of data necessary to describe the surface, which means that the polygonal surface can be used for real-time visualization of the model. Voxel models are the most precise ones, because each pixel of the 2D image is translated into a 3D voxel in a model. At the same time, the quality of the surface is very low, it has an aliasing effect and the amount of data necessary to describe the surface is large. Analytical surfaces are high-quality, but the model is difficult to reconstruct correctly.

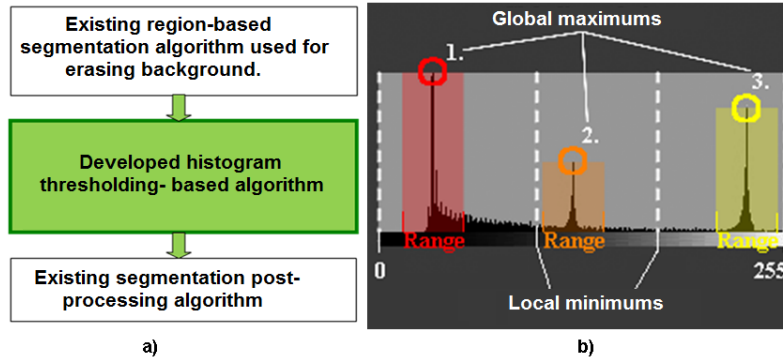
The analysis of 3D model types shows that polygonal model is better suited for 3D medical image modeling tasks, because it has such advantages as good quality, easy realization and possibility of real-time rendering.

The chapter also describes existing methods of 3D medical image construction methods. Existing methods have several disadvantages, for example, although modern tomography devices are capable of visualizing medical objects in 3D form, such systems are only installed on stations linked to the tomography system. Also, the tomography systems are expensive, and usually there are only several such systems in the hospital. But it is not always possible for physicians to effectively analyze the images of one patient on these tomography stations, while scanning of another patient takes place. On the other hand, independent medical image processing systems do not always support 3D model visualization. Therefore, it is necessary to develop a medical image processing system that could be installed on any computer in the hospital, as well as provide the necessary tools for image analysis.

### **2.3. Medical image processing and visualization methods**

This chapter describes the developed methods and their according algorithms for solving different medical image processing tasks. There are algorithms proposed for medical image segmentation, region of interest extraction, region's volume estimation, 3D visualization (control point finding algorithm and triangulation algorithm) and region's substance analysis.

**Graphic format and DICOM format image processing.** In order to provide the possibility for processing both graphic and DICOM format images an existing program ezDicom [5] was used. This is an open source program, designed for DICOM file viewing and can be used as a base for developing a medical image processing and analysis system. The program is designed to view DICOM files, although it contains no additional functions like segmentation or 3D visualization. All the developed methods were programmed using ezDicom as base program. **Semi-automatic segmentation algorithm for graphic images.** Figure 2.2.a illustrates the developed method's structure. The method combines three algorithms - one existing segmentation algorithm and one developed segmentation algorithm, based on histogram thresholding as well as one existing segmentation post processing algorithm.



2.2. fig. Developed segmentation method. a) general structure, b) histogram thresholding

*Algorithm's description:*

1. Find histogram's maximum  $m_i$  and add it to the list  $M$
2. Exclude  $m_i$  and histogram peaks within range  $(m_i - R; m_i + R)$  from further search.  $R$  is determined as follows:

$$R = \frac{255}{1.5N}, \quad (2.1)$$

where  $N$  is the defined number of maximums.

3. Search for next maximum  $m_i$
4. Repeat steps 2-3 until  $i = N$ , or  $m_i = 0$
5. Sort maximums in list in ascending order (from 0 to 255).
6. Find local minimums between maximums.
7. Define regions on histogram, each region's range lies in between local minimums (figure 2.2.b).
8. Segment the image using histogram regions.

**Semi-automatic segmentation algorithm for DICOM images.** Pathology zone extraction for DICOM format medical images is easier to realize, because of the additional information about substance density. In this case, it is possible to classify the substances (bones, gray matter, blood, etc.). It is important to develop the algorithm that would be able to segment the image, but leave the final decision, whether the region is a pathology zone to a physician.

A thresholding algorithm was selected as a base for DICOM image segmentation, because it is easy to maintain. The main idea of the method is to group pixels into segments by density. For this, several density ranges were defined as seen in table 2.2.

2.2. table. Substance density range.

Segment label	Substance	Range label	Density range, HU
$S_1$	Bones	$D_1$	400 - 1000
$S_2$	White matter	$D_2$	20 - 30
$S_3$	Gray matter	$D_3$	37 - 45
$S_4$	Water	$D_4$	0
...	...	...	...

According to this table each pixel  $p_{x,y}$  with density  $p_{HU}$  is assigned to a segment:

$$p_{x,y} \in S_i, \text{ ja } p_{HU} \in D_i \quad (2.2)$$

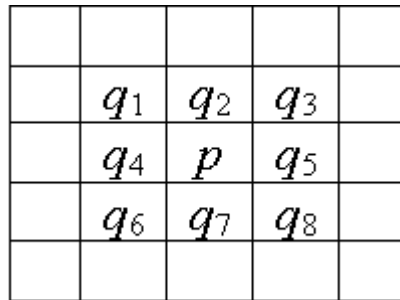
*Algorithm's description:*

1. The image is scanned horizontally, going through each image pixel.
2. If the pixel belongs to  $D_i$ , then this pixel is assigned to segment  $S_i$  that corresponds to a specific substance.
3. The second step repeats for each pixel until all pixels of the image are assigned to segments.

**Interactive region extraction algorithm for medical images.** In those cases, when the physician doesn't want to work with the segmentation map (acquired as a result of two previously described methods) or change the Hounsfield unit (HU) table to obtain a different segmentation result an interactive region extraction algorithm is proposed. In this case, the input data for the algorithm is a manually selected pixel  $p$ , which is part of a segment the user wants to extract and a substance density range  $D_i$ . The algorithm itself is a variation of a region growing algorithm [6], but the similarity criteria  $S$  is replaced by the desired regions substance density range.

*Algorithm's description:*

1. Select seed pixel  $p$ , and substance density range  $D_i$ .
2. First, the pixel  $p$  neighbor  $q_1$  is processed (figure 2.3). If  $p_{HU} \in D_i$ , then pixel  $q_1$  is added to pixel's  $p$  region.



2.3. fig. Pixel's  $p$  neighbors

3. Process next pixel's  $p$  neighbor  $q_i$  and repeat step 2.
4. When all pixel's  $p$  neighbors are processed, if some of the neighbors were added to pixel's  $p$  region then process each added pixel's  $q_i$  neighbors recursively repeating steps 2 and 3.

**Automatic region extraction algorithm for medical images.** First steps are taken in this work toward automatic pathology zone selection, although the proposed algorithm cannot be considered universal, because it does not work when the pathology zone's density is almost identical to the healthy tissue. The proposed algorithm's advantage is the possibility to save time (there's no need to process every medical image slice and select the pathology on it). The algorithm's input data is the segmentation map obtained by one of the proposed semi-automatic segmentation algorithm.

*Algorithm's description:*

1. The image is segmented using the proposed semi-automatic segmentation algorithm.
2. The image is scanned horizontally and when an unprocessed segment is found, it is labeled as processed and the algorithm checks if

$$S_{hu} \in hu_i, \quad i \in [1..n], \quad (2.3)$$

where  $S_{hu}$  – current segment's substance density,  $hu_i \in HU$ ,  $HU = \{hu_1, \dots, hu_n\}$  – pathological substance density values (blood, calcium, etc.).

3. If  $S_{hu} \in hu_i$  then the segments area is checked, if

$$S_s < 2 \cdot S_h \cdot S_w, \quad (2.4)$$

where  $S_h$  and  $S_w$  is the segments width and height, then the segment is labeled as a pathology zone.

It is necessary to check the pathology zone's area, because the pathological substance density may be found in healthy tissue as well, for example calcification can be found near the bones, but it should not be considered pathological. On the other hand, small calcification zones in the brain itself can be counted as pathology.

**Control point selection algorithm.** An algorithm is proposed for selecting control points on the extracted region's contour in order to use these points for 3D model construction. Algorithm's input data is the selected region of interest. The region is selected using the proposed segmentation and region extraction algorithms.

*Algorithm's description:*

1. First, some control points are selected as the initial adaptive contour points:
  - 1.1. A point  $P_c = (x_c, y_c)$  is found, that belongs to the extracted region. A centre of gravity may be used for this purpose:

$$P_c = \frac{\sum_{i=0}^N P_i}{N}, \quad (2.5)$$

where  $P_i$  –  $i^{\text{th}}$  point of the contour,  $N$  – number of points in contour.

- 1.2. In case the centre of gravity is outside the extracted region, a vector is drawn down from this point. When the vector reaches a point that belongs to the selected region, this point is used as  $P_c$ . If the vector does not reach such a point, it is drawn again, in opposite direction.
- 1.3. From the point  $P_c$   $M$  straight lines are drawn in clockwise motion, in such a way that the angle between those lines would be equal to  $360/M^\circ$ . The line is drawn until it reaches the border of the image and the last intersection point between the line and region's contour is considered to be the adaptive contour's point.
- 1.4. All the adaptive contour's initial points are connected with line segments forming the initial adaptive contour borders. Each point on the border is defined as:

$$\frac{(y_i - y_1)}{y_2 - y_1} = \frac{(x_i - x_1)}{x_2 - x_1}, \quad (2.6)$$

where  $x_1, y_1, x_2, y_2$  – the line segment's beginning and end points,  $x_i, y_i$  – line segment's  $i^{\text{th}}$  point.

2. For each line segment in the adaptive contour:
  - 2.1. Define threshold  $T$ , in such a way that  $T$  would be lesser if line segment is small and greater in the opposite case:

$$T = \frac{T_0}{d_0} \cdot d_{ij}, \quad (2.7)$$

where  $T_0$  – defined threshold for line segment length  $d_0$  (in experiments,  $T_0 = 1$ ),  $d_{ij}$  – length of current line segment.

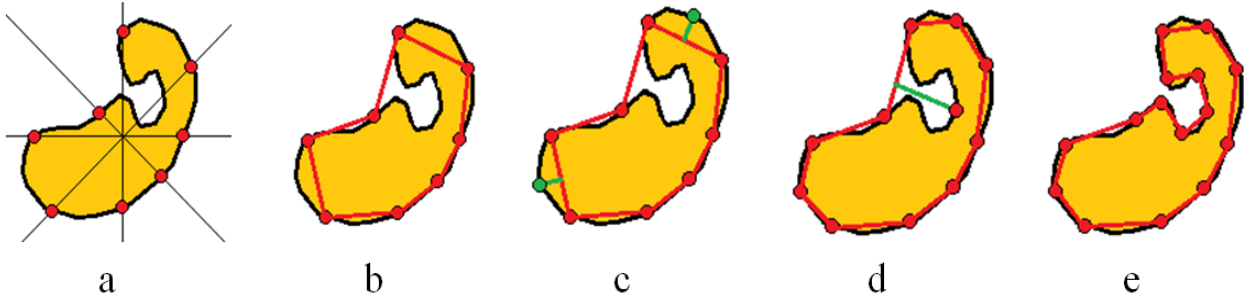
- 2.2. From line segment's each pixel draw a perpendicular vector that is directed outside the adaptive contour. When this vector reaches the region's original contour, calculate the distance between these two points according to the following equation:

$$D_i = \sqrt{(x_h - x_i)^2 + (y_h - y_i)^2}, \quad (2.8)$$

where  $x_i, y_i$  – line segment's point,  $x_h, y_h$  – original contour's point,  $D_i$  – distance.

- 2.3. Find the contour point  $(x_h, y_h)$  that is farthest from the line segment. If  $D_i > T$ , then add the point  $(x_h, y_h)$  to the adaptive contour. Else, the adaptive contour is close enough to the original contour and the next line segment is processed.
- 2.4. Repeat steps 2.1-2.3, until no more points can be added to the adaptive contour.
3. For each line segment in the adaptive contour:
- 3.1. Define threshold  $T$ , in such a way that  $T$  would be lesser if line segment is small and greater in the opposite case using equation (2.7).
- 3.2. From line segment's each pixel draw a perpendicular vector that is directed inside the adaptive contour. When this vector reaches the region's original contour, calculate the distance between these two points using equation (2.8).
- 3.3. Find the contour point  $(x_h, y_h)$  that is farthest from the line segment. If  $D_i > T$ , then add the point  $(x_h, y_h)$  to the adaptive contour. Else, the adaptive contour is close enough to the original contour and the next line segment is processed.
- 3.4. Repeat steps 3.1-3.3, until no more points can be added to the adaptive contour.
4. Repeat steps 2-3, until no more points can be added to the adaptive contour.

Figure 2.4 illustrates the steps of the algorithm and the result.



2.4. fig. a) initial adaptive contour's point selection, b) initial adaptive contour (after step 1), c) adaptive contour's growing (after step 2), d) adaptive contour's growing (after step 3), e) result

**Polygonal model and control point triangulation algorithm.** In order to successfully reconstruct the 3D model it is necessary to connect the obtained control points and create a polygonal mesh. In this case, triangulation must be used (triangular point connection, each triangle is a polygon). Since the medical object is scanned by slices, it is important to remember that only point from neighboring slices can be connected.

*Algorithm's description:*

- I. Each  $j^{\text{th}}$  point  $p_{i,j}$  of the contour on slice  $i$  is assigned a special parameter  $t_{i,j} \in (0..1)$ . The parameter  $t_{i,j}$  is calculated according to the following equation:

$$t_{i,j} = \frac{d_{i,j}}{P_i}, \quad (2.9)$$

where  $d_{i,j}$  – contour length from the  $p_{i,0}$  to  $p_{i,j}$ ,  $P_i$  – the perimeter of the contour on slice  $i$ .

The proposed method uses the control point 2D distribution. In this case, each slice  $s_i$  has  $N$  points  $p_{i,j}$ , where  $i$  – is the slice's consecutive number and  $j$  – is the point's consecutive number. Each point  $p_{i,j}$  has its own parameter  $t_{i,j}$  from 0 to 1.

II. The triangulation algorithm consecutively processes the slices in pairs. The number of control points on each slice is also taken into consideration. The slice with the greater number of control points is considered to be slice  $s_i$ . The second slice in pair is considered to be slice  $s_{i+1}$ . The pair of slices is processed in two steps::

1. Slice  $s_i$  is considered to be the base slice for the triangle polygon, i.e. there are two neighboring vertices taken from slice  $s_i$  and the third vertex is found on slice  $s_{i+1}$ .

1.1. Slice  $s_i$  neighboring points are taken as base for triangle polygon, creating following pairs:  $(p_{i,0}, p_{i,1}), \dots, (p_{i,j}, p_{i,j+1}), \dots, (p_{i,N-1}, p_{i,N})$ .

1.2. For each pair of base vertices a third one is found on slice  $s_{i+1}$ . Several conditions must be met:

1.2.1. the point's  $p_{i+1,k}$  parameter  $t_{i+1,k}$  must be different from the vertices pair normal value by no more than the given threshold  $T_t$ :

$$\left| \frac{t_{i,j} + t_{i,j+1}}{2} - t_{i+1,k} \right| < T_t, \quad (2.10)$$

where

$$T_t = 2 \cdot |t_{i,j} - t_{i,j+1}| \quad (2.11)$$

1.2.2. control point's consecutive number  $k$  must be different from the previously selected control point consecutive number  $k_{last}$  by no more than the given threshold  $T_k$ , that is dependent on the number of points  $N$  in contour:

$$|k - k_{last}| < T_k, \quad (2.12)$$

where

$$T_k = 0.01 \cdot N, \quad (2.13)$$

1.2.3. control point's distance from the vertices pair normal point  $(x_{vid}, y_{vid})$  must be minimal:

$$\sqrt{(x_{i+1,k} - x_{vid})^2 + (y_{i+1,k} - y_{vid})^2} \rightarrow \min, \quad (2.14)$$

After the first step some triangle polygons, connecting the control points will be found. Figure 2.5 illustrates the result after the first step. The gray triangles show the found polygons.



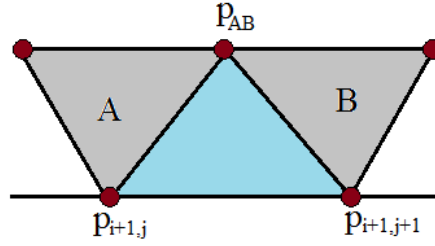
2.5. fig.. Triangulation algorithm. Result after the first step.

The second step realizes the finding of the missing connections:

2. Slice  $s_{i+1}$  neighboring points are taken as base for triangle polygon, creating following pairs:  $(p_{i+1,0}, p_{i+1,1}), \dots, (p_{i+1,j}, p_{i+1,j+1}), \dots, (p_{i+1,N-1}, p_{i+1,N})$ .

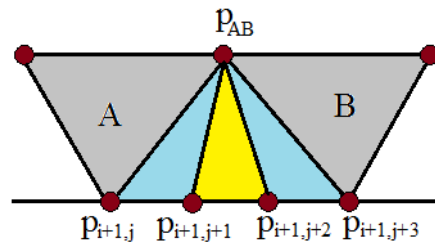
2.1. For each pair of base vertices a third one is found on slice  $s_i$ . Several conditions must be met:

2.1.1. If in the current pair both points during the first step of the algorithm were selected as third vertices for neighboring triangle polygons  $A$  and  $B$ , then the shared point  $p_{AB}$  is chosen as the third vertex (figure 2.6).



2.6. fig. Finding the third vertex

2.1.2. If in the current pair during the first algorithm's step only one or no points were chosen to be the third vertex that the third vertex is found as follows: two closest existing triangle polygons *A* and *B* are found and all the pairs between these polygons are given the point  $p_{AB}$  as the third vertex (figure 2.7).



2.7. fig. Finding the third vertex

**Volume estimation algorithm based on 2D medical image data.** The proposed method of volume estimation consists of the following steps:

First, the area of the selected region is calculated on each slice. For this, the number of pixels is counted in the region. The DICOM format contains data necessary to convert number of pixels into physical values ( $\text{mm}^2$ ).

The volume of the selected region is calculated as follows:

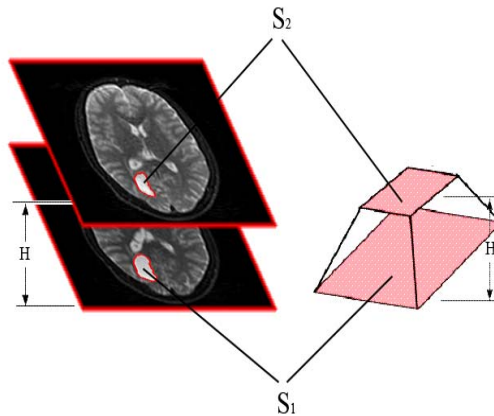
$$V = \sum_{i=1}^n v_i, \quad (2.15)$$

where  $n$  – the number of slices that contain the selected regions,  $v_i$  – volume between regions selected on neighboring slices that is calculated according to the following equation:

$$v_i = \frac{1}{3} H (S_1 + \sqrt{S_1 S_2} + S_2), \quad (2.16)$$

where  $H$  – is the distance between two slices,  $S_1$  – region's area in slice  $i$ ,  $S_2$  – region's area in slice  $i+1$ .

Figure 2.8 illustrates the calculation of volume  $v_i$ .

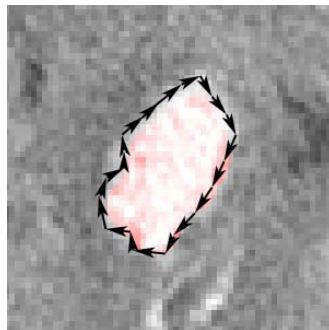


**2.8. fig. Volume  $v_i$  estimation**

**Medical image feature determination for further diagnostics.** A method is proposed that summarizes the data from medical images with the aim to provide base for further processing and diagnostics. The method analyses the substances of pathology zone and its surroundings and outputs the acquired data for the physicians to analyze.

In order to create a system that would help physicians in diagnostics it is necessary to determine the features by which the patient can be diagnosed. One of the approaches is to analyze the pathology zone's position, its substance and the substance around the pathology zone. Pathologies have characteristic features that show up on medical images in different substance densities. This means, that the comparison of medical image data to pathological features can be used to diagnose the patient. Therefore, the diagnostics procedure consists of several steps – data acquisition, data comparison with pathological features, etc. It should be noted, that the result of the comparison should not be seen as ultimate result, because even the same pathology can have different features in different patients. In this work the feature determination was considered for medical images of a brain, although the method can be used for different medical images. In this case it will be necessary to summarize pathology features that are characteristic to the specific medical image group (heart, lungs, liver, etc.).

In order to determine the substances that are positioned near the pathology zone's border it is necessary to extract the pathology zone and analyze the densities of the substances closest to the pathology zone. The pathology zone is acquired by means of segmentation and in this case the information about the pathology zone's border is also available (figure 2.9).



**2.9. fig. Pathology zone's border**

*Algorithm's description:*

1. In order to analyze the surroundings of the pathology zone it is necessary to examine the area around the border of the zone. In this case, the task is to expand the border of the

pathology zone by some step and examine the pixels that lay on the resulting border. For this, a gradient border may be found using, for example, the Sobel operator. [6]. Sobel operator is a 3x3 array (sometimes it is called convolution core or mask):

$$\begin{bmatrix} a & b & c \\ d & e & f \\ g & h & i \end{bmatrix}, \quad (2.17)$$

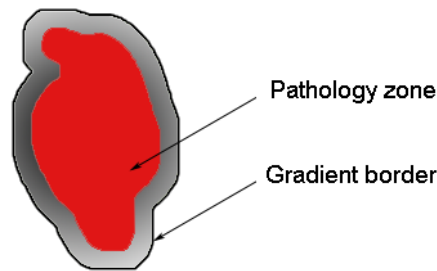
This mask is applied on the image, covering every pixel with array's element  $e$ , the mask's center. Then a gradient value is calculated. For this, a value  $S$  is calculated, using the following equation:

$$S = \sqrt{(Sx^2 + Sy^2)}, \quad (2.18)$$

where

$$\begin{aligned} Sx &= (c + 2 \cdot f + i) - (a + 2 \cdot d + g) \\ Sy &= (g + 2 \cdot h + i) - (a + 2 \cdot b + c) \end{aligned} \quad (2.19)$$

2. A threshold  $T$  is defined from 0 to 255, the greater the threshold, the greater the distance between the pathology zone and the gradient borders will be. In this work,  $T=100$ . If  $S$  is lesser than the threshold ( $S < T$ ), than the pixels is a background, else the pixel is the gradient border. The results are illustrated be figure 2.10.



**2.10. fig. Gradient border**

3. The pathology zone surroundings can now be analyzed using gradient border. In this case, the gradient border's point are arranged consecutively using square-tracing (also known as "bug") algorithm [10]. Array  $G$  is obtained as the result of the algorithm. The array consists of  $n$  elements  $g_i$  that are arranged border points. Using this array, substances are defined on this border as well as the substances percentage distribution. For this, the algorithm passes through array  $G$  and counts all the substance densities and the number of pixels for each density:

$$V_b = \sum_{i=1}^n h_i, \quad i \in [1..n], \quad (2.20)$$

where  $V_b$  – specific substance with density  $b$ ,  $h_i$  – array's  $G$  elements with density  $b$ .

The substance's  $V$  percentage distribution  $V'_b$  equals:

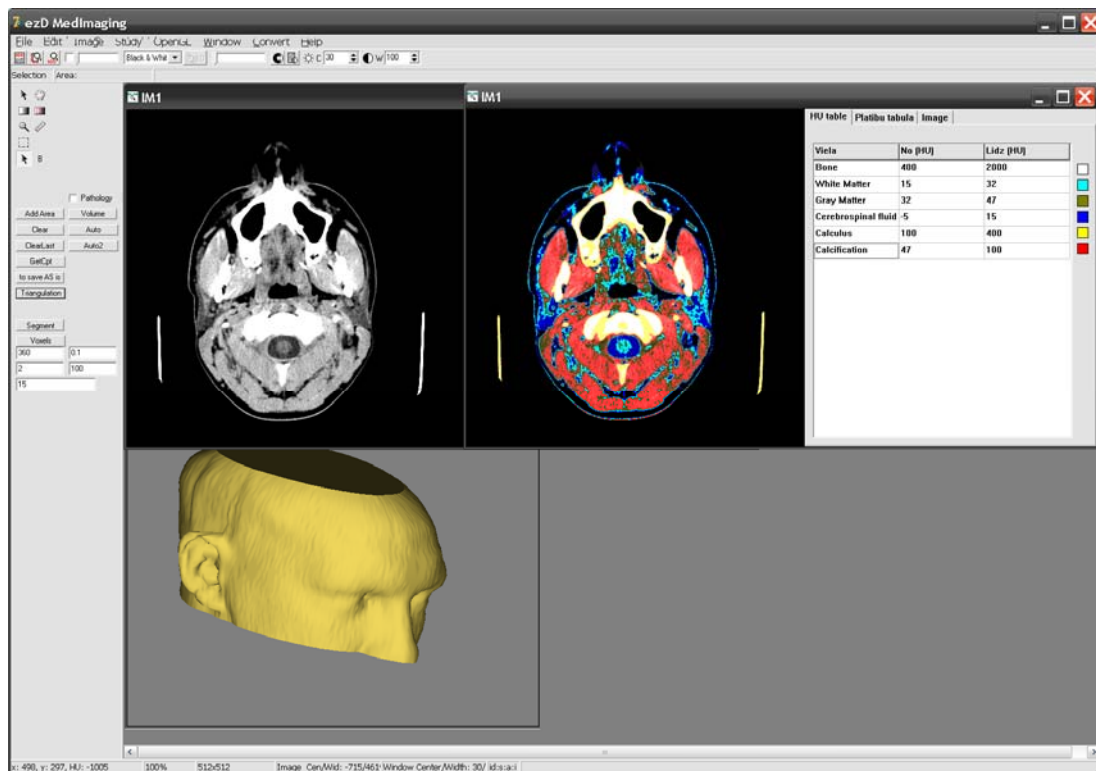
$$V'_b = \frac{V_b \cdot 100}{n}, \quad (2.21)$$

As a result, the proposed method outputs the information about the pathology zone's substance density, as well as the percentage distribution of the other substances around the pathology zone. This gives physician an opportunity to compare the obtained data with known pathological features, which may help them diagnose the patient.

## 2.4. Medical image processing methods approbation

This chapter describes the results of the experiments that were conducted with the proposed methods.

All the developed methods were summarized and combined in the developed medical image processing system. Using this developed system, experiments were conducted with the proposed methods. A screenshot of the developed medical image processing system is shown on figure 2.11.



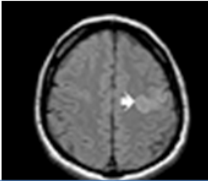
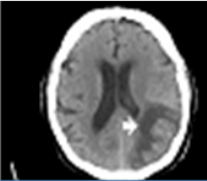
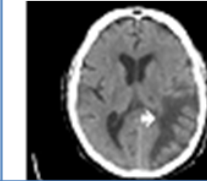
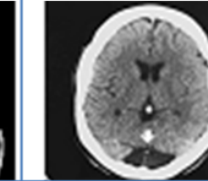
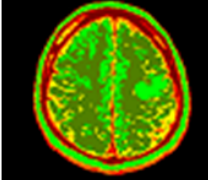
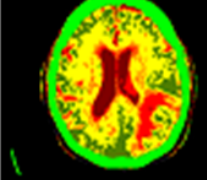
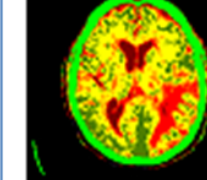
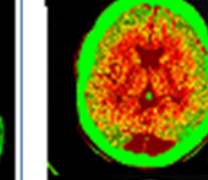
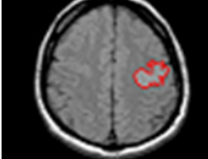
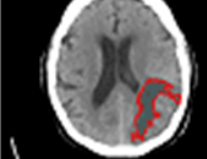
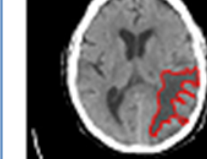
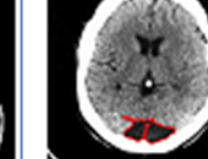
2.11. fig. The screenshot of the developed medical image processing system

The experiments were conducted with all the developed methods, including methods designed for:

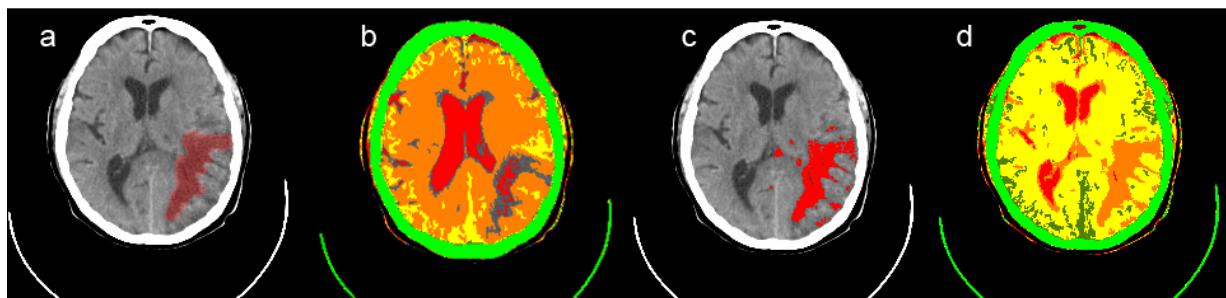
- segmentation,
- 3D visualization,
- pathology zone's volume estimation,
- analysis of the pathology zone and its surroundings.

**Semi-automatic segmentation algorithm for graphic images.** Table 2.3 shows the results of the proposed algorithm. The first row contains the original images, the white arrow shows the position of the pathology zone. The second row contains the resulting segmentation map. The third row contains the pathology zone that was extracted from the segmentation map using the proposed region extraction algorithm. The proposed method was able to segment the pathology zone on every medical image.

2.3. table. Results of segmentation

	1	2	3	4
Original images				
Proposed method's segmentation result				
Extracted pathology zone				

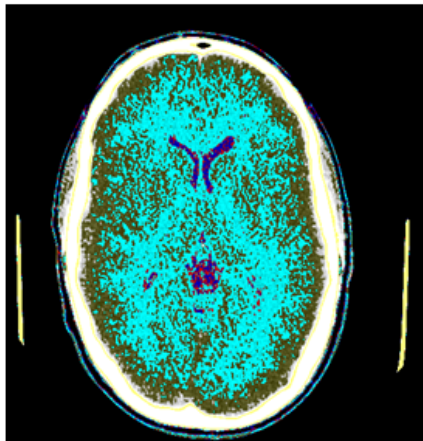
The proposed method was also compared to the existing methods – histogram thresholding-based segmentation [16] and clustering algorithm FOREL [18]. The results are shown on figure 2.12.



2.12. fig. Results of comparison. a) original image, b) existing histogram thresholding-based algorithm, c) clustering algorithm FOREL, d) proposed algorithm.

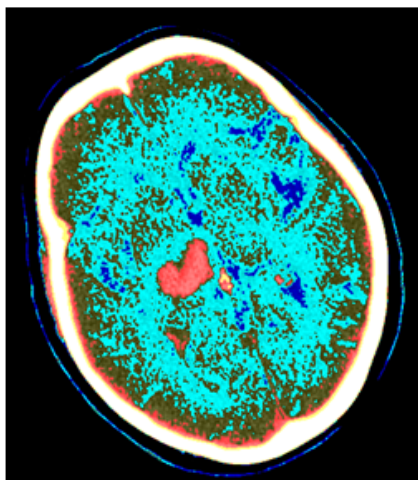
As seen from the results, the existing histogram-based thresholding algorithm is not able to fully segment the pathology zone, the clustering algorithm FOREL adds excess data to the segment. Only the proposed method was able to successfully segment the image and the pathology zone.

**Semi-automatic segmentation algorithm for DICOM images.** The results of the proposed method can be seen in figures 2.13 and 2.14. The result is output as a segmented image and a small Hounsfield unit table. The advantage of this method is the ability to see which segment contains which substance density. The Hounsfield unit table can be changed at any time, in order to correct the segmentation results for the needs of every patient.



Viela	No (HU)	Lidz (HU)
Kauli	400	2000
Balta viela	15	32
Peleka viela	32	47
Udens	-3	3
Kalcifikacija	100	400
Cerebrovask. skidr.	10	15

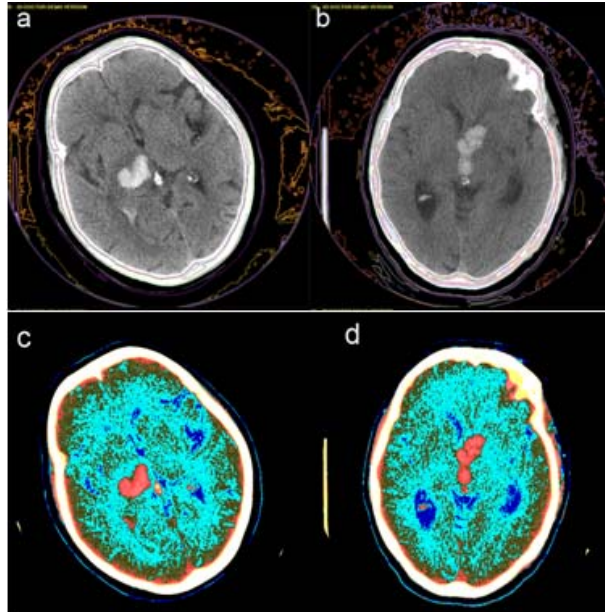
2.13. fig. Segmented medical image and its Hounsfield unit distribution table



Viela	No (HU)	Lidz (HU)
Kauli	400	1000
Balta viela	15	32
Peleka viela	32	47
Udens un CV skidr.	-5	15
Kalcifikacija	100	400
Viela ar paaug. bl.	47	100

2.14. fig. Segmented medical image and its Hounsfield unit distribution table

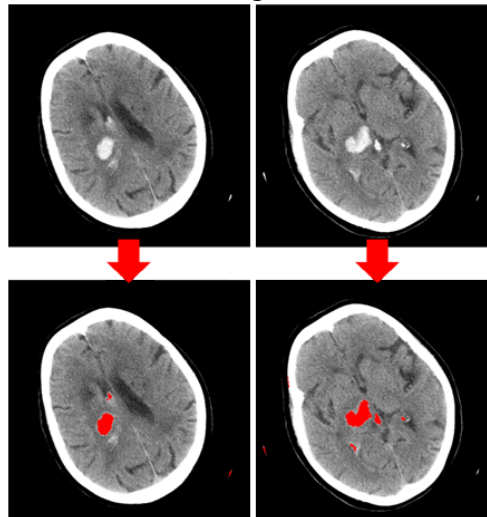
The proposed method was compared with an existing segmentation method that was realized in the medical image processing system 3D-Doctor [1]. The ability to segment the pathology zone was tested for both methods. Figure 2.15 shows the results of the tested methods. Although the existing method (fig. 2.15, a,b) was tested with different parameters, it was not able to segment the pathology zone. The proposed method (fig. 2.15 c,d) was able to segment the image and the pathology zone as well as provide additional information about segments and their substance densities.



2.15. fig. a,b) 3D-Doctor system, c,d): developed system, using the proposed segmentation method

As seen from the results, the proposed method, in contradiction to the existing systems is able to automatically segment the image according the defined density distribution table, as well as provide the information about the densities in each segment. As an additional advantage, it should be noted that the proposed method is able to segment the pathology zone clearly enough so it could be quickly selected using the interactive selection method.

**Automatic region extraction algorithm for medical images.** The method successfully finds pathology zones in medical images. After several suspicious segments were found, the user can choose any of them as a pathology zone and conduct further analysis with the acquired data. Results are shown on figure 2.16.

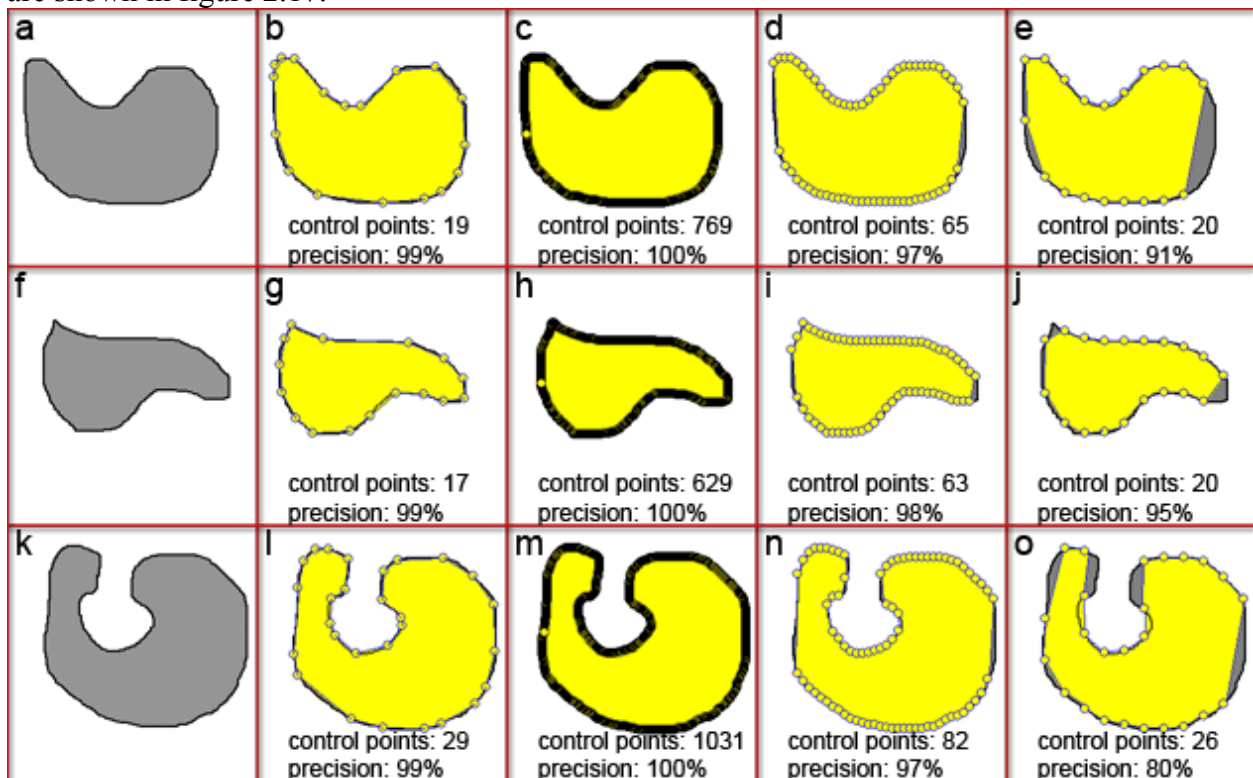


2.16. fig. Automatic region extraction

This method's precision can be enhanced by adding more criteria, i.e. check the suspicious segment's surroundings or size. For example if the segment is small, consists of water and is positioned in the gray matter, then this is normal tissue and there is no need to label it as a pathology.

**Control point selection algorithm.** The proposed method was compared to the existing square-tracing ("bug") algorithm and a scan line algorithm [10], with the aim to determine the precision and advantages of the developed method. In this case, it was

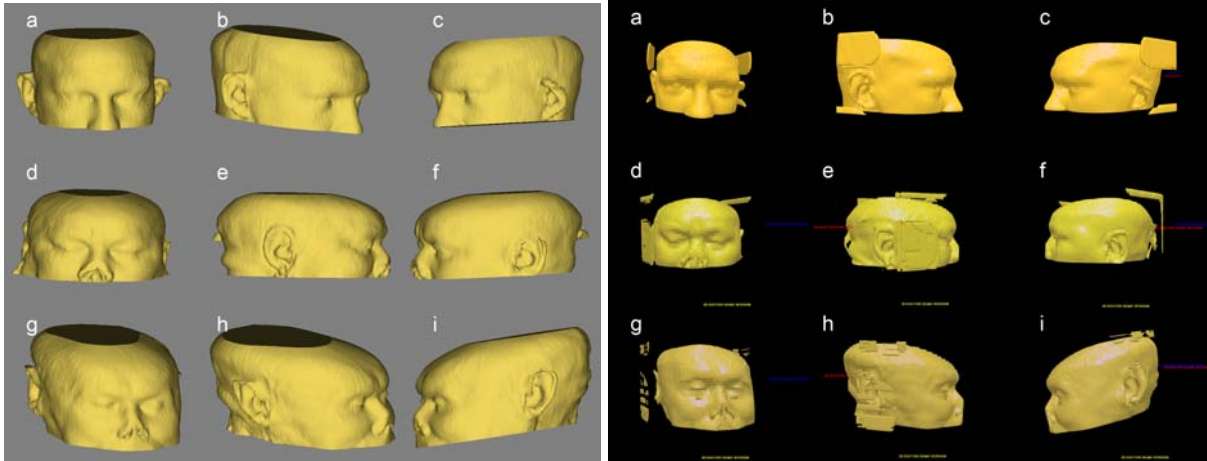
necessary to find control points on the contour in such a way so it could be precisely interpolated. The number of acquired points is also very important, because a high number of control points can slow down the visualization on a computer. The results of the experiments are shown in figure 2.17.



**2.17. fig. Control point selection algorithms results. a,f,k) original images, b,g,l) developed method, c,h,m) "bug" algorithm, d,i,n) scan line method (step = 6), e,j,o) scan line method (step = 20)**

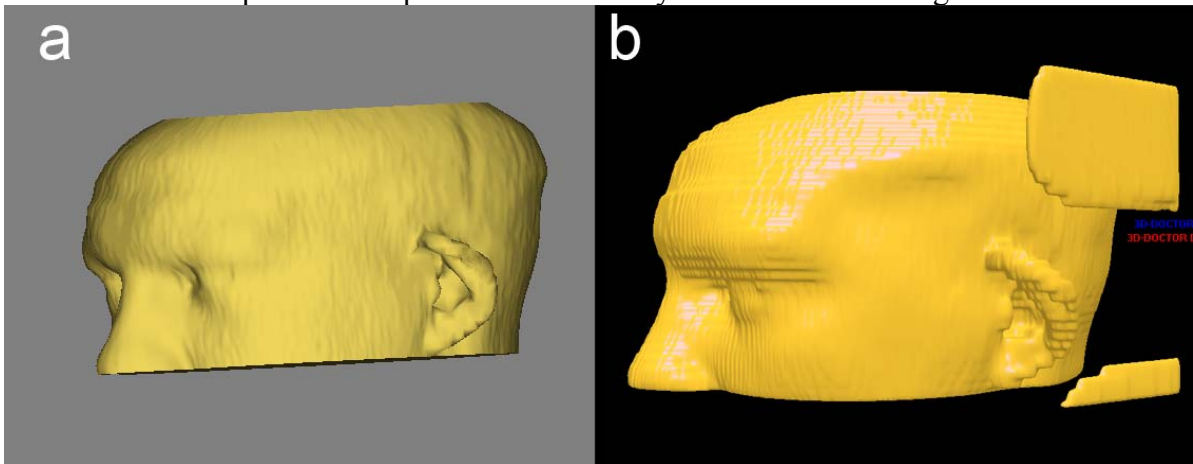
As seen from the results, the "bug" algorithm provides a high number of points even for a small region – around 1000 control points. Visualizing the rotation for a 3D model with a high number of points creates delay between frames. For example, if the data set of medical images contains 32 slices and each slice contains 1000 points, the 3D object would include 32000 points, and the computer would be able to produce roughly about 5-7 frames per second (tested on Dell Precision M4300, Intel Core 2 Duo CPU T7700 (~2.40 GHz), 2 GB RAM, NVIDIA Quadro FX 360M). Such low frame rate is very hard to work with, because it's almost impossible to set the correct object position – frames are skipped during rotation of the object. Scan line algorithm is too dependent on the selected step. If the step is too large, contour details are lost and the contour cannot be interpolated precisely. If the step is too small, this results in a high number of control points that slow down the visualization. The developed method proved its effectiveness on all the regions. The greatest advantage of the proposed method is the resulting minimum number of points necessary to interpolate the region's contour precisely and the ability to work with complex contours with concavities.

**Polygonal model and control point triangulation algorithm.** The 3D model construction algorithm (triangulation algorithm) was tested on different patient's medical images of a brain, acquired by computer tomography. In the result, the patient's face polygonal model was reconstructed using information about the skin density. The results are shown on figure 2.18 (left). The results were also compared to an existing medical image processing system 3D-Doctor [1]. The results of the 3D-Doctor system are shown on figure 2.17 (right).



**2.18. fig. left: visualization using the proposed method, right: visualization using the medical image processing system 3D-Doctor**

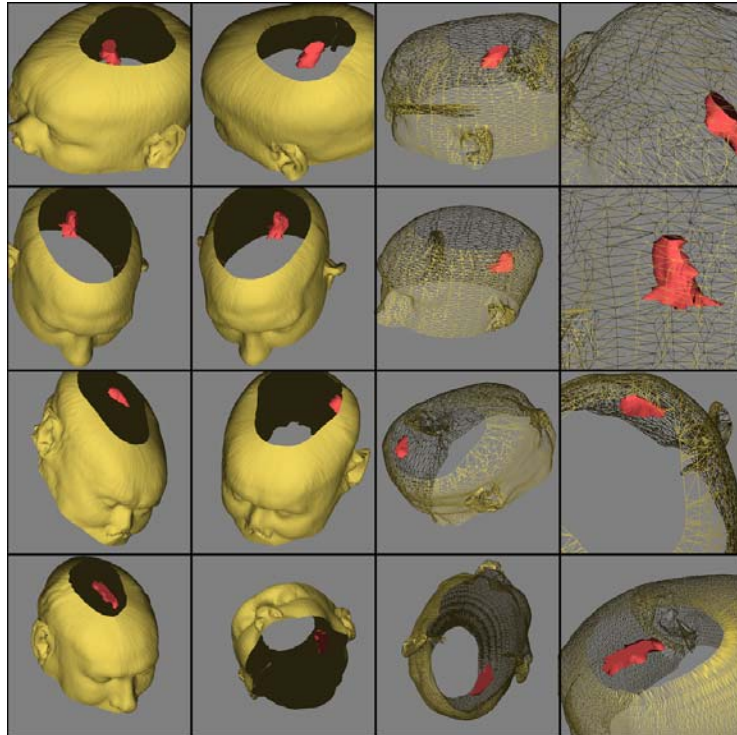
The close-up of the comparison of the two systems is shown on figure 2.19.



**2.19. fig. a) Proposed method's result, b) 3D-Doctor system's result**

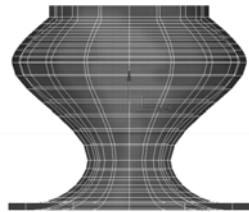
As seen from comparison, the medical object reconstructed in 3D-Doctor has an aliasing effect. The proposed method's reconstructed objects surface is smoother, the overall quality of the surface is higher, and there are no excess objects visualized in the process (like parts of the computer tomography device).

The proposed 3D visualization methods allow visualization not only of the patient's head, but also the pathology zone. This can help physicians plan necessary operations, as the position of the pathology zone inside the patient's head can be clearly seen in 3D space. Figure 2.20 illustrates that simultaneous visualization of the patient's head and the pathology zone.



2.20. fig. Patient's head and pathology zone's simultaneous visualization

**Volume estimation algorithm based on 2D medical image data.** The proposed method was compared with two existing methods – trapezoidal and Cavalieri [15]. For the input data an object with a priori known volume was used (figure 2.21). The object was sliced several times to obtain different data sets of image slices (3, 5, 7, 10) and each data set's volume was calculated using all three methods. As seen from table 2.4, the proposed method is more precise than the existing methods.



2.21. fig. Object with known volume (12141 mm<sup>3</sup>)

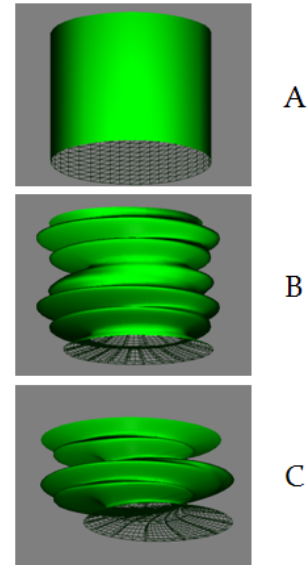
2.4. table. Experimental results

		Objects volume 12141 mm <sup>3</sup>	Cavalieri method	Trapezoidal method	Proposed method
3	slices	Volume, mm <sup>3</sup>	20461	16189	15068
	slices	Imprecision, %	69%	33%	24%
5	slices	Volume, mm <sup>3</sup>	9879	13131	13088
	slices	Imprecision, %	19%	8%	8%
7	slices	Volume, mm <sup>3</sup>	10977	13113	11554
	slices	Imprecision, %	10%	8%	5%
10	slices	Volume, mm <sup>3</sup>	11532	11846	12288
	slices	Imprecision, %	5%	2%	1%

**Volume estimation algorithm based on reconstructed 3D model.** In this work, an existing method of volume estimation (Sisojevs, 2009), described in [13,14] was approbated. The method is based on a volume estimation of a reconstructed 3D analytical model. The task

was to practically estimate the method's operation and precision. Figure 2.22 shows a table that contains experimental results. During experiments, specially modeled objects were used (figure 2.22). Volume of these objects could be precisely calculated with volume estimation methods that are based on 2D slices. All these methods give the same result on the test objects, and this calculated volume was considered to be the precise standard. Then the objects were reconstructed digitally and the volume of the obtained 3D models was estimated. As seen from the results of experiments, the imprecision for the approbated method is small and it may be used for medical image object estimation.

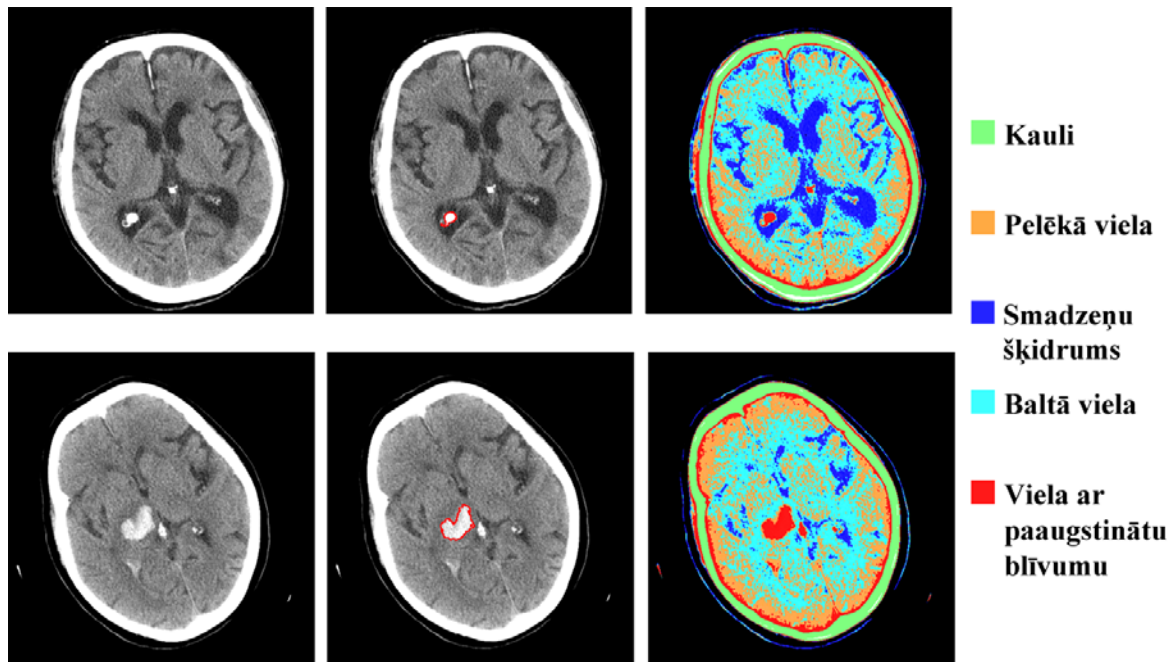
	Object A	Object B	Object C
2D Trapezoidal, Cavalieri, Proposed method. mm <sup>3</sup>	2256822	1456097	905982
	2256822	1456097	905982
	2256822	1456097	905982
3D: Approbated 3D method, mm <sup>3</sup>	2264843	1475478	922604
3D method's imprecision, %	0,36%	1,26%	1,83%



2.22. fig. Results of the proposed method

The advantage of the approbated method is the fact that it can operate with the information between medical image slices. This information is obtained by interpolating the 3D model. The 2D-based volume estimation methods lack such information, therefore it may result in imprecision when calculating more complex forms of pathologies.

**Medical image feature determination for further diagnostics.** The proposed method is able to provide information about the pathology zone substance as well as the surrounding substances. Figure 2.22 shows the experimental results. Figures from 2.22.a to 2.22.c: pathology zone's substance is a matter with heightened density (from 160 to 200 HU), surrounding substances are cerebrovascular fluid (87,2%) and white matter (12,8%). Figures from 2.22.d to 2.22.f: pathology zone's substance is a matter with heightened density (from 50 to 70 HU), surrounding substances are white matter (96,1%) and gray matter (3,9%).



2.23 fig. Data acquisition from computer tomograms

The proposed method's result is the acquired data about the pathology zone, its border and substance, as well as the information about the substances around the pathology zone. This gives physicians an opportunity to compare the obtained data with known pathological features and diagnose the patient. As seen from figure 2.3, the method precisely determined which substances surround the pathological zone.

### 3. RESULTS AND CONCLUSIONS

The doctoral thesis describes methods of medical image acquisition, existing medical image processing methods, and 3D image visualization methods. The methods are compared and analyzed and the disadvantages and problems of the existing methods are estimated. The disadvantages and problems of the existing methods define a necessity to develop new medical image processing methods and medical image processing system that would not have such disadvantages. Therefore, the aim of this work is to propose methods for medical image processing (image segmentation, region extraction, medical object's 3D construction, volume estimation of the selected region, etc.), as well as implement all the developed methods in one medical image processing system. The aim of the doctoral thesis is achieved and all the tasks are solved.

Main results of the doctoral thesis:

1. **The possibility to process medical images in both graphic and DICOM formats is insured.** In order to realize the medical image opening/saving feature an existing open source program ezDicom [5]. This open source program can be used as a basis for coding medical image processing algorithms. The program itself has limited features, allowing the opening and saving of DICOM format files, but contains no image processing and analysis tools, such as segmentation, region extraction, region's volume estimation, 3D visualization, etc.
2. **Methods for medical image segmentation and region extraction are proposed.** Methods for medical image segmentation are proposed for both graphic and DICOM images. The segmentation methods are based on histogram thresholding, region

3. **Methods for medical image 3D visualization are proposed.** In order to visualize the medical images it is necessary to solve two tasks: selection of control points on 2D medical image slices and 3D model's construction based on the acquired control points. For control point selection an adaptive contour method was developed. In contradiction to existing methods, the proposed algorithm results in a minimal number of control points necessary to precisely interpolate the region's original border. This is important for both contour correction and 3D visualization tasks. In order to visualize the medical object in 3D a polygonal model was reconstructed using the developed triangulation algorithm. The proposed 3D visualization methods has several advantages in comparison to the existing methods, such as higher surface quality, no aliasing effect and no excess segments are visualized (such as computer tomography device parts).
4. **Selected region's volume estimation method is proposed.** The proposed method of medical image volume estimation uses a data set of 2D medical images as input data. An existing method (Sisojevs, 2009) is also approbated in this work. The method is based on analytical 3D model's volume estimation. The approbated method is difficult to analyze, because it is not clear how to evaluate the acquired results. As seen from experimental results, the approbated volume estimation method is precise (the imprecision is less than 2%), but its precision is dependent on the 3D models accordance to the real object. In this work, no experiments were conducted to test this accordance, although the volume estimation of 3D models seems like a perspective scientific course. The proposed method of volume estimation based on 2D data, however, proved to be the most precise one, when compared to existing algorithms. Since the precision of volume estimation is important in medicine, only the proposed method was included in the final version of the medical image processing system.
5. **Method for medical image feature determination is proposed.** The proposed method is meant to determine the substance of the pathology zone, as well as the substances of the matters around it. The method shows the result in form of a table that contains the substance of the pathology zone and the percentage distribution of the substances around the zone. Such data may be used for diagnostics by comparing it with known pathological feature. Since different pathologies have different features it was concluded that the features could be summarized in form of rules and an expert system could be developed based on those rules. The first step, however, would be the acquirement of data about the pathology zone and the developed algorithm is aimed to solve this task.

In total, different methods for various medical image processing tasks are proposed in the doctoral thesis. All the proposed algorithms were approbated by attending the scientific conferences and the experimental results were published in scientific publications.

The main accomplishment of the doctoral thesis is the developed medical image processing system that is based on the proposed image processing algorithms. The system was positively evaluated by the dean of Faculty of Medicine from Riga Stradina University and Gailezers hospital Radiology department director prof., Dr.med. A. Platkajis. The

developed system is able to solve the problems of accessibility and medical image analysis that medical experts have with the current equipment and software. This allows physicians to diagnose the patient as quickly as possible and that is important for timely diagnosis. The developed medical image processing system and the proposed methods were compared with an existing medical image processing system 3D-Doctor and it was concluded that the developed system has several advantages over the 3D-Doctor, such as:

- the segmentation algorithm's result is easier to understand and analyze,
- there is a possibility to automatically segment the pathology zone,
- the medical objects 3D visualization has higher quality,
- there is a possibility to evaluate volume of the medical object.

## REFERENCES

- [1] Able Software Corp. 3D-Doctor, FDA 510K Cleared, Vector-Based 3D Imaging, Modeling and Measurement Software / Internets. - <http://www.ablesw.com/3d-doctor/index.html>
- [2] Aminah A.M., Wan E., Arsmah I., Rozi M., Siti S.Y., Abdul K.J. Region and Boundary Segmentation of Microcalcifications using Seed-Based Region Growing and Mathematical Morphology // *Procedia - Social and Behavioral Sciences*, Volume 8, 2010, pp. 634-639
- [3] Bilgic S., Sahin B., Sonmez O.F., Odaci E., Colakoglu S., Kaplan S., Ergur H. A new approach for the estimation of intervertebral disc volume using the Cavalieri principle and computed tomography // *Clinical Neurology and Neurosurgery*, Volume 107, Issue 4, June 2005, pp. 282-288
- [4] Dastidar P., Heinonen T., Vahvelainen T., Elovaara I. and Eskola H. Computerised volumetric analysis of lesions in multiple sclerosis using new semi-automatic segmentation software // *Medical and Biological Engineering and Computing*, 1999, Volume 37, Number 1, pp. 104-107
- [5] ezDICOM DICOM viewer / Internets. - <http://www.cabiatl.com/mricro/ezdicom/>
- [6] Forsyth D.A., Ponce J.. *Computer Vision: A Modern Approach*, Prentice Hall, US, 2002
- [7] He L., Peng Z., Everding B., Wang X., Han C.Y., Weiss K.L., Wee W.G. A comparative study of deformable contour methods on medical image segmentation // *Image and Vision Computing*, Volume 26, Issue 2, 1 February 2008, pp. 141-163
- [8] Lai C.-C., Chang C.-Y. A hierarchical evolutionary algorithm for automatic medical image segmentation // *Expert Systems with Applications*, Volume 36, Issue 1, January 2009, pp. 248-259
- [9] Odaci E., Sahin B., Sonmez O.F., Kaplan S., Bas O., Bilgic S., Bek Y., Ergü H. Rapid estimation of the vertebral body volume: a combination of the Cavalieri principle and computed tomography images // *European Journal of Radiology*, Volume 48, Issue 3, December 2003, pp. 316-326
- [10] Pavlidis T. *Algorithms for Graphics and Image Processing*, Computer Science Press, Rockville, Maryland, 1982
- [11] Pichel J.C., Singh D.E., Rivera F.F. Image segmentation based on merging of sub-optimal segmentations // *Pattern Recognition Letters*, Volume 27, Issue 10, 15 July 2006, pp. 1105-1116
- [12] Sandor T., Metcalf D., Kim Y.-J. Segmentation of brain CT images using the concept of region growing // *International Journal of Bio-Medical Computing*, Volume 29, Issue 2, November 1991, pp. 133-147

- [13] Sisojevs A., Glazs A. Volume Estimation of 3D Object Modelled by Parametrical Iso-Surfaces. // Biomedical Engineering. Proceedings of International Conference, Kaunas University of Technology, October 2010, pp. 220-224
- [14] Sisojevs A., Krechetova K., Glazs A. 3D Modeling of Free-Form Object (Interpolation, Visualization and Volume Estimation), The 17th International Conference on Computer Graphics, Visualization and Computer Vision WSCG'2009 Communication Papers proceedings. – Plzen: University of West Bohemia, 2009, pp. 125-128
- [15] Smitha S., Revathy K., Kesavadas C.. Segmentation and Volume Estimation of Brain tissues from MR Images, Proceedings of International MultiConference of Engineers and Computer Scientists, June 2006, pp. 543-547
- [16] Taheri S., Ong S.H., Chon V.F.H. Level-set segmentation of brain tumors using a threshold-based speed function // Image and Vision Computing, Volume 28, Issue 1, January 2010, pp. 26-37
- [17] Wu Y. Image Segmentation: The First Step In 3-D Imaging, 1999
- [18] Загоруйко Н. Г., Ёлкина В. Н., Лбов Г. С. Алгоритмы обнаружения эмпирических закономерностей. Новосибирск: наука, 1985